AIMS Environmental Science

AIMS Environmental Science, 11(1): 21–37.
DOI: 10.3934/environsci.2024002
Received: 10 December 2023
Revised: 07 January 2024
Accepted: 24 January 2024
Published: 05 February 2024

http://www.aimspress.com/journal/energy

Research article

Preparation and development of amidoxime-modified Fe_3O_4/SiO_2 core-shell magnetic microspheres for enhancing U(VI) adsorption efficiency from seawater

Alif Alfarisyi Syah, Anugrah Ricky Wijaya* and Irma Kartika Kusumaningrum

Department of Chemistry, Faculty of Mathematics and Sciences, Universitas Negeri Malang, Jl. Semarang 5 Malang 65145, Indonesia

*** Correspondence:** Email: anugrah.ricky.fmipa@um.ac.id.

Abstract: We synthesized and characterized amidoxime-modified Fe_3O_4/SiO_2 core-shell magnetic microspheres tailored for maximal U(VI) sorption efficiency from seawater. Through meticulous structure and spectroscopy analyses, the microspheres, which were designed with amidoxime functionality, exhibited remarkable U(VI) sorption capabilities compared to raw silica-coated Fe_3O_4 counterparts. The maximum percent uranium adsorption (98.57%) was achieved at 60 minutes with 0.05 g of adsorbent, using a synthetic solution of 25 mg L^{-1} $UO_2(CH_3COO)_2$. $2H_2O$ at pH 7 and 25 ºC (298 K). The kinetic studies highlighted rapid equilibrium achieved within 1 hours. Following the pseudo-second-order model, the microspheres reflected a maximum sorption capacity of 24.286 mg g^{-1} at pH 7 and 298 K. The U(VI)-loaded microspheres could be efficiently separated via an external magnetic field with adsorption efficiency of 91.67% at pH 6.5 and efficiently regenerated by HCl, indicating their potential for U(VI) preconcentration and separation from seawater. This research contributed to the development of high-performance sorbents for U(VI) removal and holds promise for solving the radioactive element elimination and enrichment, performing its stability, selectivity, and reusability across multiple cycles.

Keywords: amidoxime; magnetic; uranium; adsorption

1. Introduction

Uranium, which occurs mostly in the form of U(VI) in the environment, has enormous strategic and ecological significance amidst global challenges. Dwindling fossil fuel reserves and the urgent need to combat climate change have led many countries to turn to nuclear power as an alternative energy source, increasing their dependence on uranium [1,2]. This increasing demand has driven ongoing efforts to extract uranium from diverse and unconventional resources, including seawater. However, the massive release of uranium into the environment due to nuclear activities poses a significant long-term threat to ecosystems and organisms. Regulatory bodies such as the World Health Organization impose strict limits on uranium concentrations in drinking and spring water, underscoring the urgent need for highly effective uranium recovery from aqueous solutions. Researchers have carried out exploration of heavy metals to investigate anthropogenic and natural sources of metals in marine waters [3,4]. Therefore, designing efficient and sustainable uranium extraction methods becomes important not only for energy security but also for environmental protection[5]

Adsorption method has emerged as a promising technique due to its simplicity, cost-effectiveness, and wide applicability. The search for new adsorbent materials with attributes such as high surface area, fast adsorption kinetics, and pH stability has gained significant traction. Recent studies demonstrating the potential of nanomaterials, such as nano oxides, nanocarbons, and carbon-based nanocomposites, have revealed their extraordinary absorption capabilities. However, challenges remain in efficiently separating these sorbents from the post-saturation water phase, thereby limiting their scalability for treating larger volumes of water [6,7]. Magnetic nanoparticles (MNPs), especially Fe_3O_4, are promising but have limitations such as susceptibility to oxidation, leaching in acidic conditions, and aggregation in solution, thereby affecting their absorption capacity [8,9].

To address these challenges, extensive attention has been devoted to modifying MNPs' surfaces through physical coating or covalent binding. For instance, Humid–acid–coated Fe_3O_4 nanoparticles have proven efficient in removing Eu(III)[10], and Pb(II)[11]. Similarly, Chitosan-coated Fe_3O_4 nanoparticles exhibited a notable capability in extracting Cu(II)[12]. SiO_2 emerges as an optimal shell constituent owing to its stability, resistance to redox reactions, and ample surface hydroxyl groups[13]. Amidoxime, renowned for its amphoteric qualities and strong affinity for U(VI), has displayed exceptional performance in modifying substrates to facilitate efficient U(VI) recovery[14]. Utilizing amidoxime, this research has adapted core–shell Fe_3O_4 to produce amidoxime-modified Fe_3O_4/SiO_2–AO. This material shows promising potential in extracting U(VI) from aqueous solutions, accompanied by investigation of uptake kinetics, geochemical effects, uptake capacity, stability, and regeneration. These findings provide valuable insights in evaluating the application potential of Fe_3O_4/SiO_2–AO for effective U(VI) recovery and removal, especially from unconventional sources such as seawater. This emphasizes the role of surface-modified magnetic microspheres as a viable solution to address these pressing challenges. By focusing on improving absorption efficiency and stability, we aim to bridge the gap between the increasing demand for uranium and the urgent need for environmentally friendly extraction techniques, thereby paving the way for sustainable energy practices and ecological preservation.

In this study, Fe_3O_4 coating with silica can be carried out using the sol-gel method and amidoxime functionalization as research Zhao et al, (2013)[15]. The effect of Amidoxime on the characteristics of Fe_3O_4/SiO_2-AO nanocomposites were also observed. Characterization of Fe_3O_4, Fe_3O_4/SiO_2, and Fe_3O_4/SiO_2-AO nanocomposites using Fourier transform infrared (FT-IR) to identify functional groups, detailed information about the crystallographic structure used X-Ray diffraction analysis (XRD), and

measurement the magnetization used Vibrating-sample magnetometry (VSM) methods. Uranium adsorption is carried out, including variations in the amount of adsorbent and contact time to find the its kinetics by Fe_3O_4/SiO_2-AO nanocomposites[16]. The uranium concentration test was carried out using the UV-Vis Spectrometer method, was chosen because there are already many of them people have used it since the first time introduced by Currah and Beamish, (1948)[17].

2. Experimental details

2.1. Materials

$FeCl_3 \cdot 6H_2O$, $FeSO_4.7H_2O$, ethanol, NH_4OH, $SnCl_2$, H_2SO_4, HCl, and 5N HNO_3 were provided by Duta Jaya Laboratory Supply (Indonesia). NH_4SCN was produced by Phy Edumedia Malang (Indonesia). Tetraethyl orthosilicate (TEOS) and glutaraldehyde (Glu) were produced by Nitrakimia Laboratory Supply (Indonesia). 3–aminopropyl triethoxysilane (APS), K_2CO_3, $NH_2OH \cdot HCl$, Diaminomaleonitrile (DAMN 99%), and $UO_2(CH_3COO)_2.2H_2O$ were purchased from Chemical Laboratory Supply SIP Malang (Indonesia). All reagents were of analytical purity and used without further purification.

2.2. Methods

2.2.1. Preparation of Fe_3O_4 Nanoparticles

The Fe_3O_4 nanoparticles were synthesized using a procedure similar to a prior study[9]. A mixture of 75 mL of 0.19 M $FeSO_4 \cdot 7H_2O$ solution and 75 mL of 0.25 M $FeCl_3 \cdot 6H_2O$ solution were mixed in a 250 ml beaker glass. The mixture was heated to a temperature of 90 °C, and added 10 mL of 25% NH_4OH solution. This solution was stirred for 30 minutes using a magnetic stirrer. The resulting black precipitate was filtered using distilled water until it reached a neutral pH of 7. The precipitate was subsequently dried in an oven at a temperature of 50-60 °C for a duration of 5 hours. To achieve homogeneity, the obtained solids were ground using a mortar and pestle.

$$2Fe^{3+}(aq) + 6OH^-(aq) \rightarrow 2Fe(OH)_3(s)$$

$$Fe^{2+}(aq) + 2OH^-(aq) \rightarrow Fe(OH)_2(s)$$

$$2Fe(OH)_3(s) + Fe(OH)_2(s) \rightarrow Fe_3O_4(s) + 4H_2O(l)$$

Figure 1. Synthesis results of Fe_3O_4 nanomagnetite applied with magnet external.

2.2.2. Preparation of Fe_3O_4/SiO_2

The synthesis of Fe_3O_4/SiO_2 microspheres with a core/shell structure was conducted using sol-gel method [18]. In a typical procedure, 1 g of the Fe_3O_4 particles prepared earlier were dispersed in a solution containing ethanol (100 mL), water (25 mL), and NH_4OH (2.5 mL) through ultrasonication for 30 minutes. Furthermore, 6 mL of TEOS was slowly added drop by drop, and the reaction was left to progress for 5 hours with continuous stirring. The resulting product was gathered via centrifugation, washed thoroughly with distilled water and ethanol multiple times, and then dried under vacuum conditions at 60 °C for 6 hours.

2.2.3. Preparation of Fe_3O_4/SiO_2–AO

a. Fe_3O_4/SiO_2-APS

A total of 0.5 gram of Fe_3O_4/SiO_2 microspheres were immersed in 50 mL of ethanol. Subsequently, 0.2 ml of APS was mixed and refluxed at 70 °C for 16 hours. After that, the resulting product was centrifugated, washed with both distilled water and ethanol, and finally dried under vacuum conditions at 60 °C for 6 hours.

b. Fe_3O_4/SiO_2-APS-Glu

The solid Fe_3O_4/SiO_2-APS-Glu obtained earlier was dispersed in a solution containing 1.1 mL of glutaraldehyde mixed with 100 mL of ethanol at room temperature. It was then stirred continuously for 3 hours to facilitate the–presence of the aldehyde group. The released product was collected, centrifuged, and rinsed by water and ethanol.

c. Fe_3O_4/SiO_2-APS-Glu-DAMN-AO

Fe_3O_4/SiO_2-APS-Glu was immersed in a solution containing 0.5 g Diaminomaleonitrile (DAMN), which is dissolved in 100 mL of ethanol at room temperature for 3 hours. The resulting solid Fe_3O_4/SiO_2-APS-Glu-DAMN was isolated and purified. Subsequently, it was added with 1.0 g K_2CO_3 and 1.0 g $NH_2OH{\cdot}HCl$ dissolved in 100 mL of ethanol for 6 hours at 70 ^oC within a sealed flask. The produced Fe_3O_4/SiO_2–AO was retrieved via centrifugation, followed by washing with distilled water and ethanol. The mixture was then dried and conducted under vacuum conditions at 60 ^oC. The synthesis process is outlined schematically in Figure 3.

Figure 2. Fe_3O_4/SiO_2–AO nanocomposite applied in an external magnetic field.

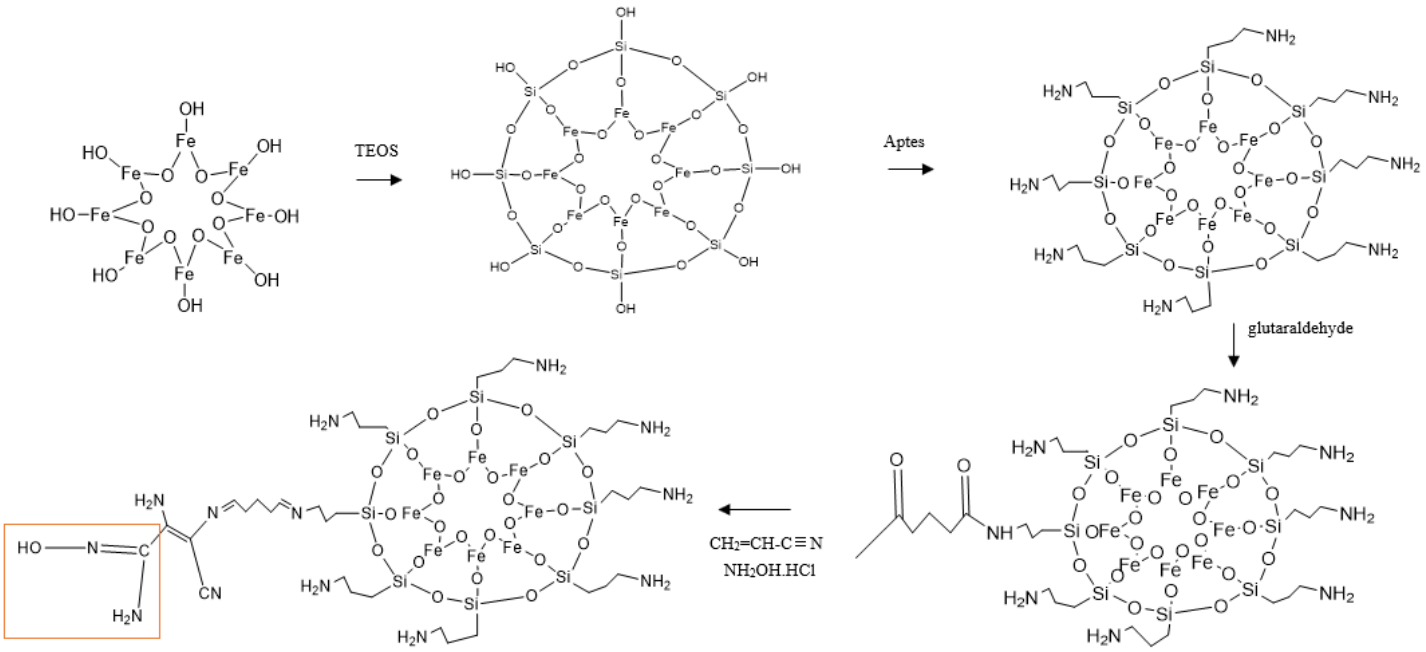

Figure 3. Schematic illustration of the preparation procedure of Fe_3O_4/SiO_2–AO.

2.3. Characterization of Fe_3O_4 Nanoparticles and Fe_3O_4/SiO_2-AO Composites.

The initial characterization of the Fe_3O_4 and Fe_3O_4/SiO_2-AO nanoparticles involved employing a Fourier transform infrared spectrometer (FT-IR, Shimadzu IR Prestige 21) to identify the compounds' functional groups. Subsequently, X-ray diffraction (XRD, PANalytical X'Pert Pro) was utilized to assess their crystallinity, while vibrating-sample magnetometry (VSM, DXV-100~550 Series) was employed to determine the magnetic moment.

2.4.Uranium analysis

2.4.1. Calibration Curve Preparation

The uranium was analyzed by UV-Vis using the Ascorbic Acid and Stannous Chloride Methods reagent. A 2000 ppm uranium solution was taken 50 mL and diluted to 1000 ppm. Then, 2.5; 5; 10; and 25 mL were taken from the solution to make uranium solutions with concentrations of 25, 50, 100, and 250 ppm. Each solution was added with 5 drops of concentrated HCl, 15 mL of distilled water, 8 mL of 8 M NH_4SCN solution, and 2 mL of 10% $SnCl_2$ solution. The solutions were diluted, left for ±30 minutes for color formation.

2.4.2. Preparation and measurement of sample solutions

Sample solution of uranium was taken 5 mL and added to a 25 mL volumetric flask. To each volumetric flask, 5 drops of concentrated HCl (including the blank), 15 mL of distilled water, 8 mL of 8M NH_4SCN solution, and 2 mL of 10% $SnCl_2$ solution were added. The solution was then eluted with distilled water up to the mark. The solution was homogenized by shaking and left for approximately 30 minutes before measuring using UV-Vis spectroscopy at a wavelength of 380 nm.

2.5. Adsorption Experiment

The uranium adsorption was investigated through batch experiments. Initially, different quantities of Fe_3O_4/SiO_2-AO nanocomposites 0.01 g, 0.02 g, 0.05 g, 0.075 g, and 0.1 g were placed into separate Erlenmeyer flasks. Subsequently, 50 mL of a 25 mg L^{-1} uranyl acetate solution was added to each flask. These Erlenmeyer flasks were then agitated at 150 rpm for one hour at neutral pH and room temperature. The primary objective of this experiment was to determine the optimal amount of adsorbent needed for effective uranium adsorption. To establish the ideal contact time between the adsorbent and adsorbate, the contact time variation was initiated, ranging from 5 to 85 minutes. Furthermore, the solution was filtrated using Whatman 42 filter paper to separate the nanocomposite from the solution. The filtered sample was analyzed to determine the uranium concentration by UV-Vis spectroscopy at a wavelength of 380 nm. The calculated of the uranium adsorbed onto the Fe_3O_4/SiO_2-AO was used in the designated formula, as follows:

$$\text{Adsorption \%} = \frac{Co-Ce}{Co} \text{ x } 100 \quad (1)$$

$$q_e = \frac{(Co-Ce) \text{ x } V}{m} \quad (2)$$

q_e (mg g^{-1}) shows the adsorption capacity, *C*o (mg L^{-1}) and *C*e (mg L^{-1}) show the uranium concentration before and after the adsorption process, m (g) and V (L) show the amount of adsorbent, and the volume of the solution, respectively.

2.6. Regeneration and stability experiments

The regeneration was determined through desorption experiments, where a given mass of 0.02 g of adsorbents was thoroughly rinsed and dispersed in 0.05L of 0.1 M HCl solutions and shaken at 150 rpm for 60 min at 299.5 K. After magnetic separation, the remaining U(VI) concentration in the supernatant was measured to evaluate the desorption percentage. The regenerated Fe_3O_4/SiO_2-AO was washed thoroughly with distilled water and then used for the next sorption–desorption cycle. Additionally, the leached Fe concentration in the supernatant was determined by UV-Vis spectroscopy based on complex Fe^{2+} 1,10-Phenanthroline. The desorbing agents used in this study included HCl (0.1 M and 1.0 M) to determine the stability of Fe in Fe_3O_4/SiO_2-AO. The calculated of efficiency percent uranium adsorption and desorption to the Fe_3O_4/SiO_2-AO were used in the designated formula, as follows:

$$\text{Adsorption Efficiency \%} = \frac{q_e}{C_o} \text{ x 100} \quad (3)$$

$$\text{Desorption Efficiency \%} = \frac{C_d}{C_o} \text{ x } 100 \quad (4)$$

C_d (mg L-1) show the uranium concentration after the desorption process.

3. Results and discussion

3.1. Characterization of Fe_3O_4, Fe_3O_4/SiO_2, and Fe_3O_4/SiO_2-AO Nanocomposites

The XRD analysis of the Fe_3O_4 nanoparticles and Fe_3O_4/SiO_2-AO nanocomposites were conducted by comparing the diffraction peaks with those of pure Fe_3O_4 obtained from the Crystallography Open Database (COD) with ID number 1011032. All the diffraction peaks coincided with those of the cubic phase of the Fe_3O_4, with peak positions at 2θ: 18.25°, 30.18°, 35.55°, 43.20°, 53.57°, 57.15°, and 62.78°, corresponding to (111), (220), (311), (400), (422), (511), and (440) planes of the Fe_3O_4. The XRD pattern of the the Fe_3O_4/SiO_2-AO nanocomposite showed a decrease in the diffraction intensity, all the Fe_3O_4 diffraction angles, and a broad peak at 2θ = 22°, which is associated with amorphous silica[19]. No other crystal peaks were detected, indicating the absence of other crystalline phases.

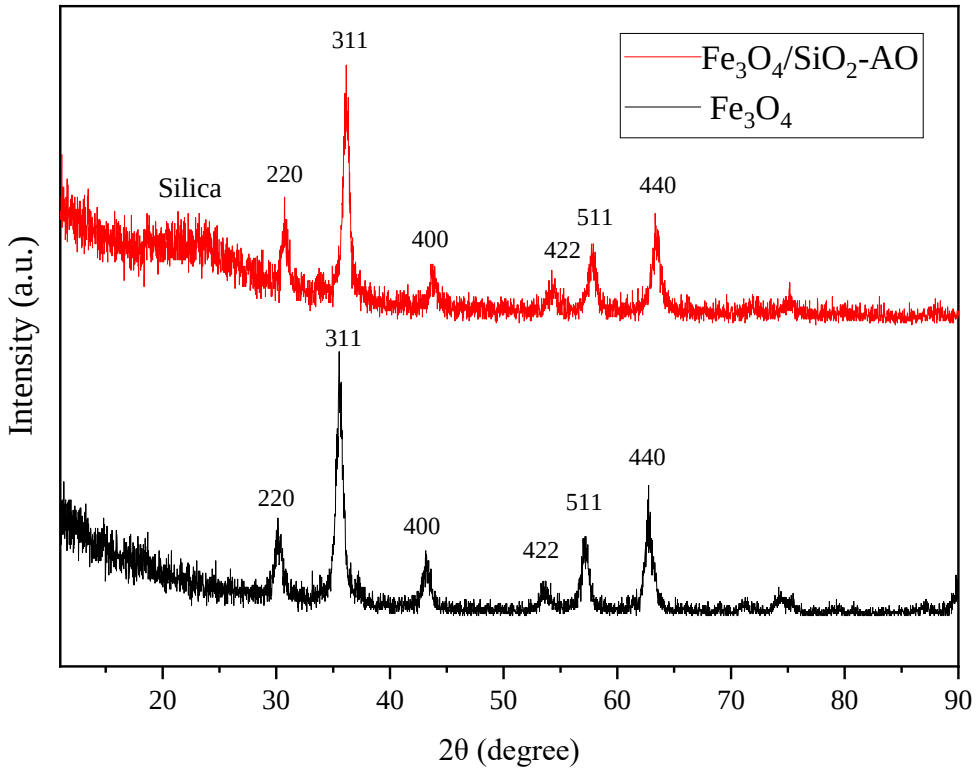

Figure 4. XRD Patern of Fe_3O_4 and Fe_3O_4/SiO_2-AO Nanocomposites.

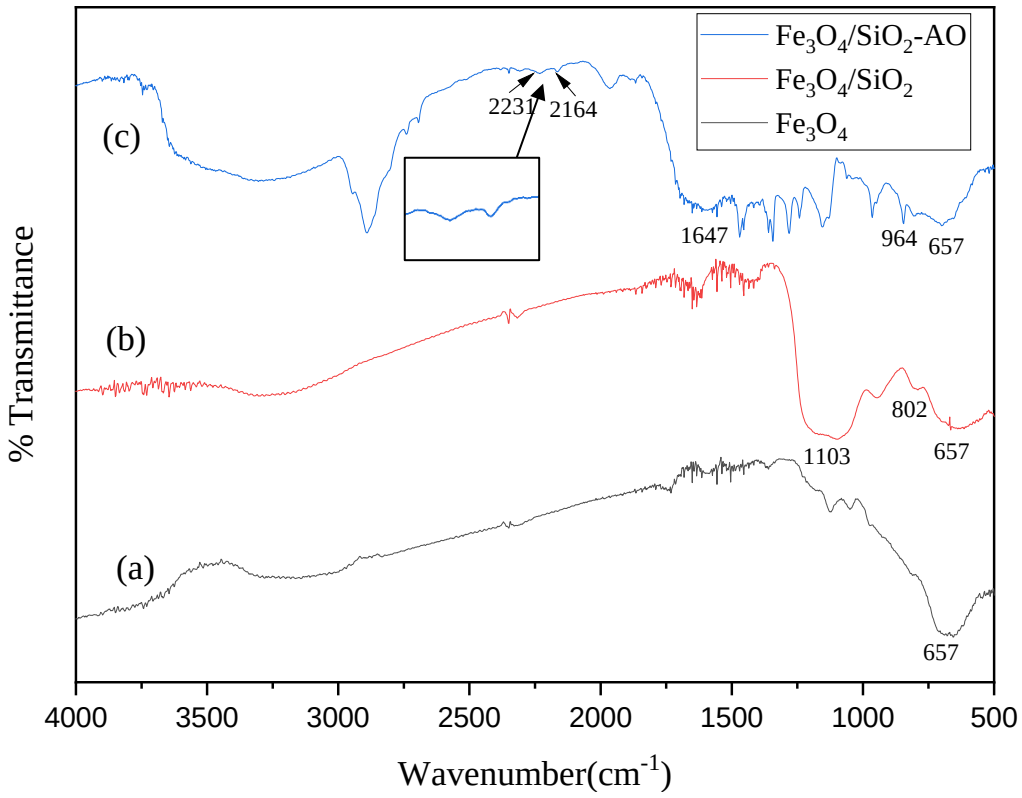

Figure 5. The infrared spectra of (a) Fe_3O_4, (b) Fe_3O_4/SiO_2, and (c)Fe_3O_4/SiO_2-AO Nanocomposites.

The FT–IR spectra of Fe_3O_4, Fe_3O_4/SiO_2, and Fe_3O_4/SiO_2-AO were examined to detect any changes due to the amidoxime functional group modification, as shown in Figure 5. The peak observed at 657 cm^{-1} signifies the stretching vibration of the Fe–O bond (Figure 5a). Additionally, a broad band ranging from 802 cm^{-1} to 1103 cm^{-1} indicates the Si–O–H and Si–O–Si [19] stretching vibrations. It showed the presence of a silica coat on the magnetite surface (Figure 5b). Figure 5c shows that there's slight bands emerging at 2164 cm^{-1} and 2231 cm^{-1}, signaling the C≡N stretching vibration. An intriguing observation is the split of the C≡N absorption band into two peaks, potentially due to the differing chemical environments of the two C≡N groups post in the condensation reaction [20]. On the Fe_3O_4/SiO_2-AO spectrum (Figure 5c), the C=N absorption registers at 1647 cm^{-1} and 964 cm^{-1}, representing the C=N and N–O stretching vibrations specific to the amidoxime groups, respectively [21].

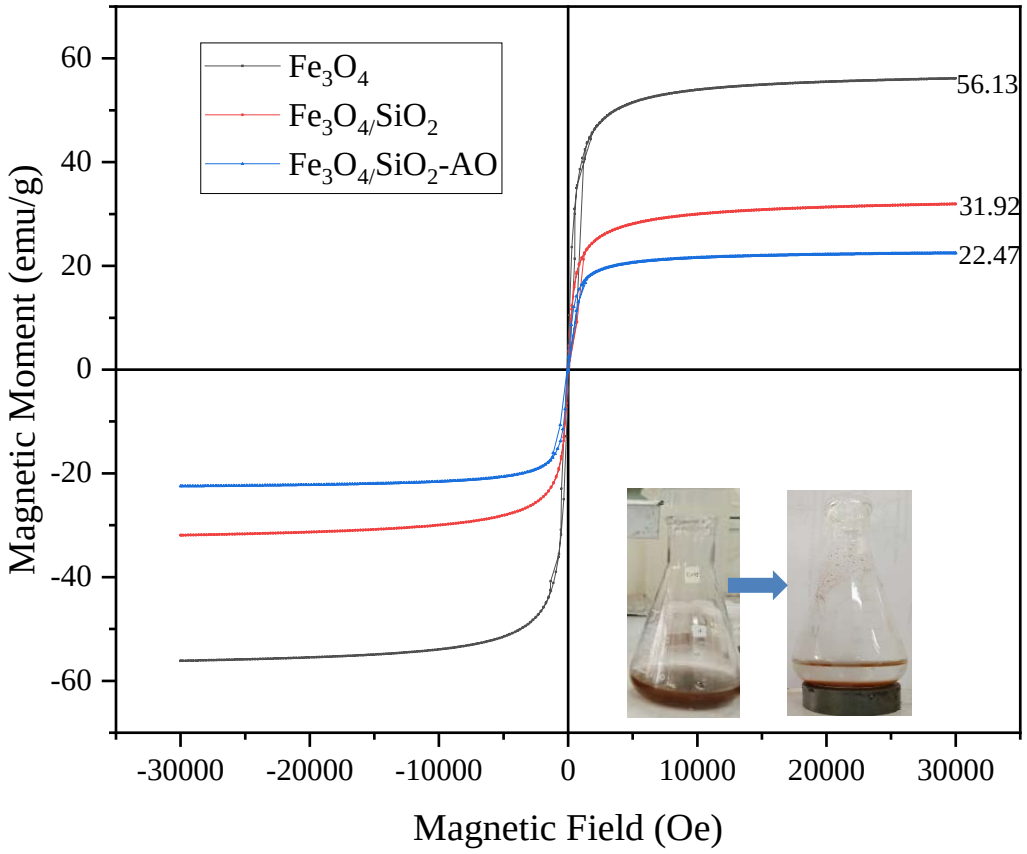

Figure 6. Hysterical curve of (a) Fe_3O_4, (b) Fe_3O_4/SiO_2, and (c)Fe_3O_4/SiO_2-AO nanocomposites.

The magnetic characteristics of Fe_3O_4, Fe_3O_4/SiO_2, and Fe_3O_4/SiO_2-AO were analyzed through magnetization curves at room temperature (Figure 6). This curve shows no hysteresis loops, indicating the superparamagnetic behavior of both materials. The saturation magnetization (Ms) values were measured at 56.13, 31.92, and 22.47 emu g^{-1} for Fe_3O_4, Fe_3O_4/SiO_2 and Fe_3O_4/SiO_2-AO, respectively. Although there was a decrease in saturation magnetization due to a low magnetite content after a layer of non-magnetic mesoporous silica and amidoxime was covered by the nanomagnetic surface. However, the separation of Fe_3O_4/SiO_2-AO was easily separated from the reaction medium using an external magnet. Thus, it is possible to reuse the nanocomposite in the adsorption-desorption process. Pourgazi et al, 2017 reported that the magnetic material which has an Ms value of around 22 emu g^{-1} shows a sufficient magnetic response as an adsorbent [22]. Magnetic separation can be achieved completely within 1 min by placing a magnet near the vessel containing the Fe_3O_4/SiO_2-AO suspension (Figure 6).

3.2. Uranium Analysis with Ascorbic Acid and Stannous Chloride Methods

During the staining process, the thiocyanate ion reacts with the uranyl ion in an acidic environment. The yellow color from the uranyl thiocyanate complex remained stable for 48 hours. This method is suitable for determining uranium (VI) concentrations ranging from 4 to 40 mg L^{-1} [23]. The addition of concentrated HCl to both the standard and sample solutions is intended to ensure a pH below 1. It is necessary to prevent the hydrolysis of the $SnCl_2$ solution. After adding concentrated HCl, it was added immediately 15 mL of distilled water to prevent the decomposition of the NH_4SCN

solution. The decomposition of $SnCl_2$ and NH_4SCN solutions can lead to errors in color intensity and must be avoided. Measurements of standard, sample, and blank solutions are taken after allowing the staining solution to react for approximately 30 minutes. During measurements, standard blank and sample blank solutions are required to correct for any absorption from the blank solution matrix. The results of measurements on standard solutions with concentrations of 25, 50, 100, and 250 mg L^{-1} are used to create a calibration curve as presented in Figure 7. As listed in Table 1, the absorbance values of standard points provide data for constructing the calibration curve shown in Figure 7. This figure reveals a linear relationship between absorbance and concentration (R^2 value of 0.9925).

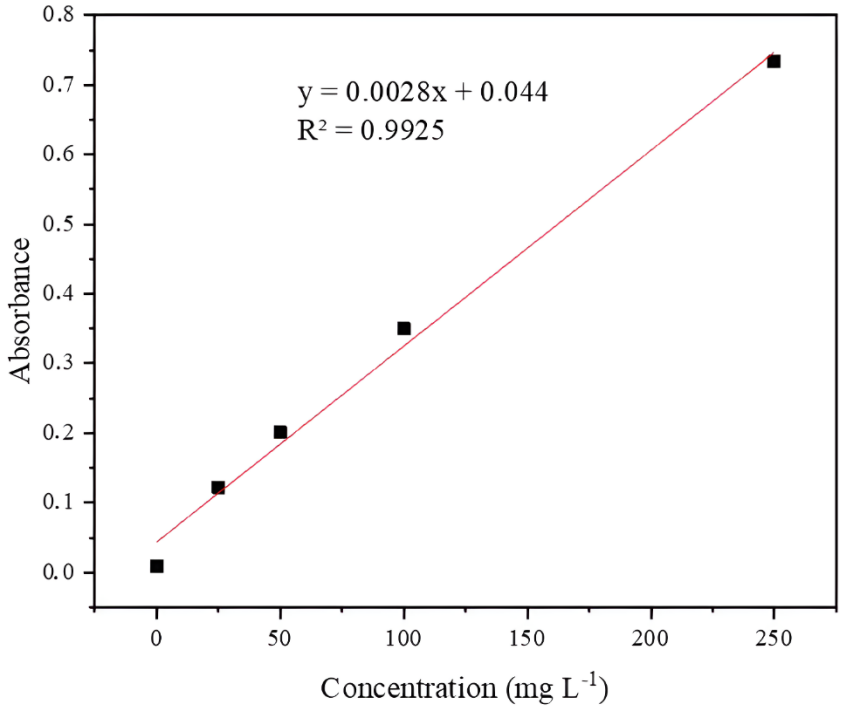

Figure 7. The Calibration Curve of Uranium Analysis.

3.3. Application of Uranium Adsorption

The efficacy of uranium adsorption is directly related to the quantity of adsorbent used. Employing a dose of 0.05 g of adsorbent led to an impressive 98.57% uranium adsorption efficiency. The increasing of mass adsorbent correlated with the ability more active sites significantly enhancing the uranium adsorption capacity of the Fe_3O_4/SiO_2-AO-nanocomposites. However, the effect of the adsorbent dose on the uptake of U(VI) shows that with an increase in the adsorbent dose within the range of 0.01–0.05 g/L. Further increase of the adsorbent dose from 0.05 to 0.075 g/L would lead to a reduction in the removal percentage, possibly due to the decline of specific surface area and active sites due to adsorbent nanoparticle aggregation[24].

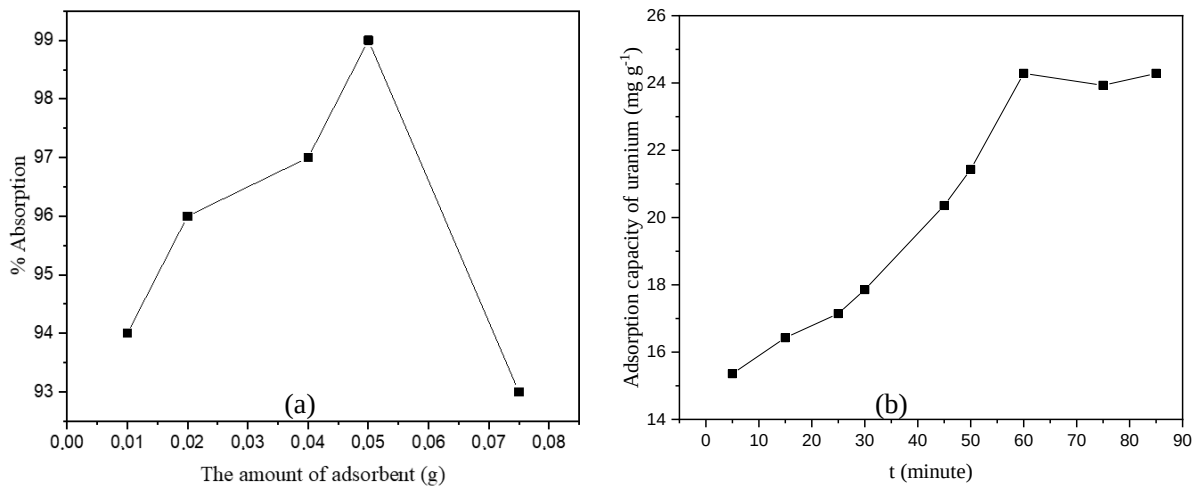

Figure 8. Influence of the amount of adsorbent (a); contact time (b).

The impact of contact duration on uranium absorption by Fe_3O_4/SiO_2-AO nanocomposites is under examination, as depicted in Figure 8b. It clearly illustrates that absorption levels rise with prolonged contact time. The peak absorption occurred after 60 minutes, followed by a decline in absorption at the 75-minute. The highest equilibrium adsorption capacity for uranium stood at 24.286 mg g^{-1} at 60 minutes, and then diminished to 23.929 mg g^{-1} at 75 minutes. This indicates that the adsorbate molecules are not completely binding to the active sites of the adsorbent due to saturation, resulting in partial detachment and subsequent reduction after the optimum period. This further suggests that the increasing contact time caused the available surface area to decrease, impacting the adsorbent's ability to capture uranium molecules. Moreover, the rate of uranium molecule release increases until it stabilizes. This indicates that the adsorbent has reached its optimal contact time.

3.4. Adsorption Kinetic of Uranium

We continued to investigate the uranium adsorption kinetics by Fe_3O_4/SiO_2-AO nanocomposites ranging from 5 to 85 minutes. Both the pseudo-first-order and pseudo-second-order kinetic models were applied. The indicators such as q_t (mg g^{-1}) and q_e (mg g^{-1}) track the quantity of absorbed uranium at specific time intervals and at equilibrium, respectively. The rate constants, k_1 (min^{-1}) and k_2 (g/mg·min), integral to the pseudo-first-order and pseudo-second-order kinetic equations, are derived by examining the gradient of the natural logarithm of (q_e - q_t) against time (t) and the intercept of the graph [25], as shown in the Figure 9. The data analysis regarding with the initial concentration, final concentrations at specific intervals, and its equilibrium concentration was determined to find the most suitable kinetics model. These experiments were conducted at 25 ºC (298 K), commencing with an initial uranium concentration of 25 mg L^{-1} in a 50 mL solution, utilizing Fe_3O_4/SiO_2-AO nanocomposites weighing 0.05 g, as listed in Table 1.

Pseudo-first-order equation: $$ln(q_{e-}\ q_t\ ) = lnq_{e-}\ k_1 t \quad (5)$$

Pseudo-second-order equation: $$\frac{t}{q_t} = \frac{1}{K_{2\ q_e^2}} + \frac{1}{q_e} \quad (6)$$

Table 1. Experimental results at 25 ºC (298 K), contact time ranged 5-85 minute.

Time (min)	*C*t (mg L^{-1})	*q*t (mg g^{-1})	log (q_e-q_t)	*t*/*qt*
0	25	0	1.385	0
5	9.64	15.357	0.951	0.326
15	8.57	16.429	0.895	0.913
25	7.86	17.143	0.854	1.458
30	7.14	17.857	0.808	1.680
45	4.64	20.357	0.594	2.211
50	3.57	21.429	0.456	2.333
60	0.71	24.286	-	2.471
75	1.07	23.929	0.252	3.333
85	0.71	24.286	-	2.471

In this investigation, the uranium adsorption kinetics were observed to conform to a pseudo-second-order model (Figure 9b). The linear regression coefficient (R^2) suggests that the pseudo-second-order kinetics model offers a more appropriate explanation for the uranium adsorption process involving Fe_3O_4/SiO_2-AO nanocomposites (Table 1). This implies that prolonged contact between the nanocomposites and uranium ions results in an increased ratio of time to capacity. Consequently, the influence of valence forces on the shared electron utilization between the adsorbent surface and organic molecules impacts the adsorption rate.

Table 2. Kinetic parameters of uranium adsorption by Fe_3O_4/SiO_2-AO based on Pseudo-first order and Pseudo-second order.

Metal Ions	Pseudo-first order				Pseudo-second order		
	$q_{e,exp}$	$q_{e,cal}$	K_1 (min-1)	R^2	$q_{e,cal}$	K_2 (g/mg·m)	R^2
U(IV)	24.286	11.541	0.024	0.910	22.624	8.33E-03	0.981

The q_e value calculated using the second-order pseudo model was almost close to the experimental q_e value ($q_{e,exp}$), while the correlation coefficient (R^2) of the first-order pseudo model was lower than that of the second-order pseudo model. This shows that the experimental data agree better with the simulation data of the pseudo-second-order model than with the pseudo-first-order model. These results strongly suggest that the dominant mechanism controlling the rate of U(VI) adsorption by Fe_3O_4/SiO_2-AO indicating the strong surface complexation or chemical adsorption.

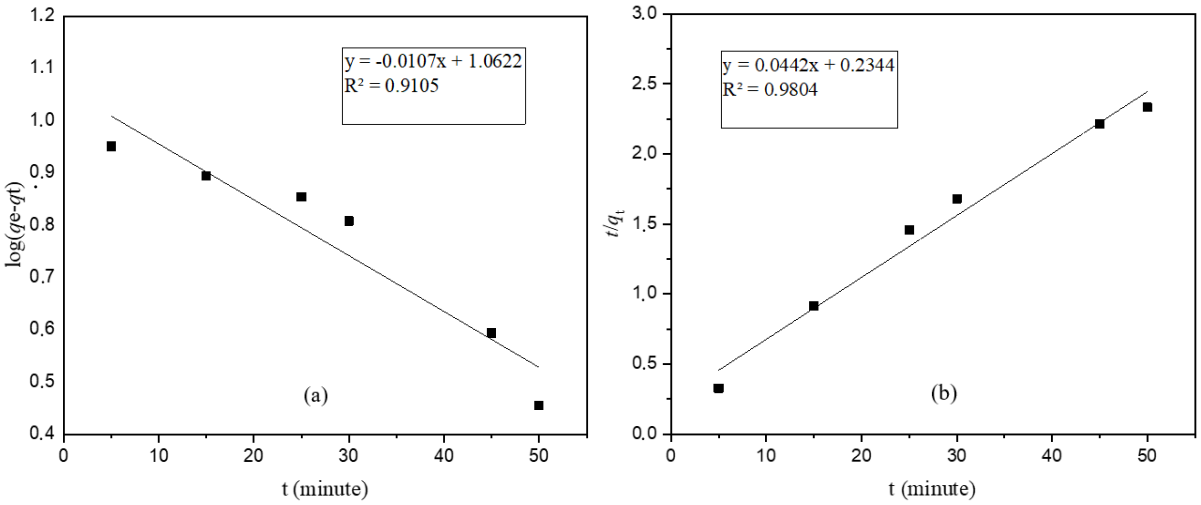

Figure 9. Adsorption kinetics curves (a); pseudo-first-order; (b) pseudo-second-order.

3.5. Applications of Uranium Adsorption in Seawater

The seawater used in this research was taken in the sea area of the south coast of Prigi Bay and the collection location refers to Wijaya et al, (2019) [26,27]. They reported the seawater quality was within the WHO threshold. Evaluation of the performance of the adsorbent Fe_3O_4/SiO_2-AO in uranium adsorption was carried out in two pH conditions at pH in the located sampling and at pH 10. The adsorption was carried out during the optimum contact time with a simulated seawater solution spiked with 25 mg L^{-1} uranium. The uranium concentration before and after adding 25 mg L^{-1} spike solution was obtained at 0.357 mg L^{-1} and 22.42 mg L^{-1}.

Table 3. Uranium adsorption efficiency in seawater with adsorbents Fe_3O_4/SiO_2-AO.

pH	C_o (mg L^{-1})	C_e (mg L^{-1})	q_e (mg g^{-1})	AE %
6.5	22.42	1.79	19.64	92.01
10	22.42	3.21	18.21	85.68

Notes: AE means Adsorption Efficiency.

As listed in Table 3, the adsorbent has of 92.01% AE at pH 6.5 and decreased to 85.68% at pH 10. This indicates the effect of pH on the interaction between the adsorbent surface and the uranium species in solution. At pH 10, the deprotonation of functional groups in the nanocomposite is more significant, creating a more negatively charged surface, which increases the interaction between negatively charged surfaces to form noncomplex species such as $UO_2(OH)^{3-}$ and $UO_3(OH)^{7-}$ in solution. However, at very high pH, U(VI) hydrolysis becomes more significant, producing U(VI) species that cannot be complexed, causing electrostatic repulsion between the negatively charged nanocomposite and the also negatively charged uranyl ions, leading to decreased adsorption performance. At pH 6.5, deprotonation of some functional groups of the nanocomposite slightly reduces the repulsion between the negatively charged surface and uranium ions, facilitating absorption[20,28].

3.6. Regeneration and stability studies

The regeneration of sorbents is a crucial aspect in evaluating their potential environmental and economic impact. In the study by Zhao et al, (2014)[29] amidoxime-functionalized magnetic mesoporous silica microspheres were synthesized for selective sorption of U(VI). The amount of U(VI) absorption is suppressed under acidic conditions, thus indicating that acid treatment is carried out for regeneration of U(VI)-loaded Fe_3O_4/SiO_2-AO. The study shows that Fe_3O_4/SiO_2-AO has potential as a candidate for selective separation of U(VI) from aqueous solutions in possible real applications on seawater.

Table 4. Regeneration and reuse cycles of Fe_3O_4/SiO_2-AO in the sorption of U(VI)

Adsorption-desorption and reuse cycles	C_o (mg L^{-1})	C_e (mg L^{-1})	q_e (mg g^{-1})	C_d (mg L^{-1})	AE %	DE %
1	22.42	0.36	22.06	20.357	98.41	92.27
2	22.42	2.15	20.28	15.71	90.44	77.49
3	22.42	1.79	20.63	15.36	92.04	74.42
4	22.42	2.14	20.27	14.64	90.44	72.21

Notes: DE means Desorption Efficiency.

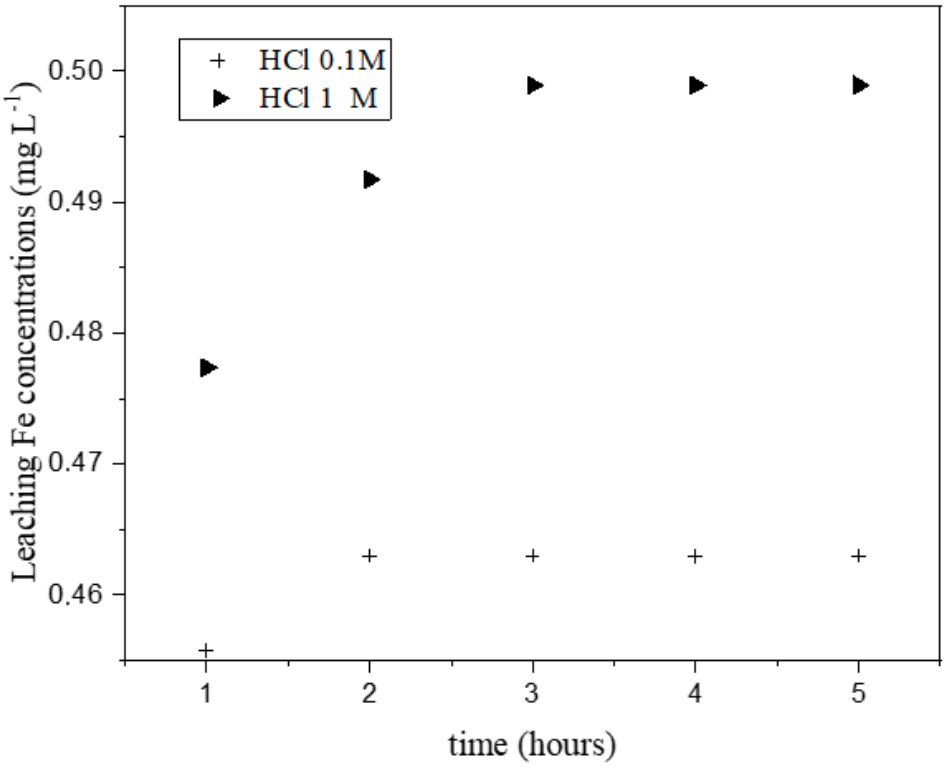

Figure 10. Effect of HCl concentration on Fe Leaching.

The study investigates the regeneration of Fe_3O_4/SiO_2-AO nanocomposite for U(VI) adsorption using spiked original seawater samples and 0.1 mol·L^{-1} HCl. The results show that the nanocomposite

has a high EA level of 90.44-98.41% the four absorption cycles, indicating its good performance for U(VI) adsorption. The U(VI) desorption from the Fe_3O_4/SiO_2-AO surface in the first cycle was 92.27% and slightly decreased in cycles 2-4 was 77.49-72.21% (%RSD=3.55). Moreover, the adsorption capacity remains constant with still suggests a high level of regeneration and reuse. The stability of Fe_3O_4/SiO_2-AO under acidic conditions was evaluated by monitoring the amount of Fe leaching after different contact times with HCl concentrations (0.1-1M). The results demonstrate that the amount of Fe leaching within 1–5 hours is largely inhibited in acidic solutions due to the success of the SiO_2 coating and the high stability of Fe_3O_4/SiO_2-AO under acidic conditions.

4. Conclusions

The successful synthesis of Fe_3O_4/SiO_2-AO nanocomposites involved the efficient extraction of SiO_2 from TEOS sand and amidoxime. These nanocomposites exhibited a variety of functional groups Fe-O, Si-O-Si, Si-OH, C=N, OH^-, and NH_2 that proved advantageous in facilitating the adsorption process. After its optimization, the ideal conditions for uranium adsorption by these nanocomposites were determined using 0.05 g of adsorbent with a contact time of 60 minutes. We obtained the maximum percent uranium adsorption was at 98.57%. The adsorption process was well-explained by pseudo-second-order models, highlighting their effectiveness in describing uranium adsorption in to Fe_3O_4/SiO_2-AO nanocomposites. Furthermore, Fe_3O_4/SiO_2-AO loaded with uranium can be conveniently separated from water solutions using a magnet external and adsorption efficiency uranium in seawater of 92.01% at pH 6.5 and efficiently regenerated by HCl. The straightforward process, quick action, and efficient sorption capabilities of Fe_3O_4/SiO_2-AO holds promise as a remarkably efficient material for extracting and recovering uranium from polluted wastewater and seawater.

Use of AI tools declaration

The authors declare not used Artificial Intelligence (AI) tools in the creation of this article.

Acknowledgments

The authors are grateful to the (DRTPM) Thesis Master Research Grant 2023. We express their gratitude to the editor and reviewers for their comments to improve the manuscript significantly.

Conflict of interest

The authors stated that there is no conflict of interest for the study.

References

1. Plant JA, Simpson PR, Smith B, et al. (1999) Uranium ore deposits - Products of the radioactive earth. *Rev Mineral Geochem* 38: 254–319. https://doi.org/10.1515/9781501509193-011
2. Waltar AE, Reynolds AB (1983) Fast Reactors. *Nucl Power Technol* 1: 297–333.

3. Wijaya AR, Ouchi AK, Tanaka K, et al. (2012) Metal contents and Pb isotopes in road-side dust and sediment of Japan. *J Geochem Explor* 118: 68–76. https://doi.org/10.1016/j.gexplo.2012.04.009
4. Wijaya AR, Kusumaningrum IK, Hakim L, et al. (2022) Road-side dust from central Jakarta, Indonesia: Assessment of metal(loid) content, mineralogy, and bioaccessibility. *Environ Technol Innov* 28: 102934. https://doi.org/10.1016/j.eti.2022.102934
5. Rao TP, Metilda P, Gladis JM (2006) Preconcentration techniques for uranium(VI) and thorium(IV) prior to analytical determination-an overview. *Talanta* 68: 1047–1064. https://doi.org/10.1016/j.talanta.2005.07.021
6. Buszewski B, Szultka M (2012) Past, Present, and Future of Solid Phase Extraction: A Review. *Crit Rev Anal Chem* 42: 198–213. https://doi.org/10.1080/07373937.2011.645413
7. Wijaya AR, Khoerunnisa F, Armid A, et al. (2022) The best-modified BCR and Tessier with microwave-assisted methods for leaching of Cu/Zn and their $\delta^{65}Cu/\delta^{66}Zn$ for tracing sources in marine sediment fraction. *Environ Technol Innov* 28.
8. Khatamian M, Divband B, Shahi R (2019) Ultrasound assisted co-precipitation synthesis of Fe_3O_4/ bentonite nanocomposite: Performance for nitrate, BOD and COD water treatment. *J Water Process Eng* 31: 100870. https://doi.org/10.1016/j.jwpe.2019.100870
9. Nanlohy F, Wijaya AR, Semedi B (2021) Synthesis of Fe_3O_4/MnO_2/Humic acid nanocomposite for strontium ion adsorption and its interferences, *AIP Conference Proceedings*, 030108. https://doi.org/10.1063/5.0052981
10. Yang S, Zong P, Ren X, et al. (2012) Rapid and highly efficient preconcentration of Eu(III) by core-shell structured Fe_3O_4/Humic acid magnetic nanoparticles. *ACS Appl Mater Inter* 4: 6891–6900. https://doi.org/10.1021/am3020372
11. Liu JF, Zhao ZS, Jiang G Bin (2008) Coating Fe_3O_4 magnetic nanoparticles with humic acid for high efficient removal of heavy metals in water. *Environ Sci Technol* 42: 6949–6954. https://doi.org/10.1021/es800924c
12. Chang YC, Chen DH (2005) Preparation and adsorption properties of monodisperse chitosan-bound Fe3O4 magnetic nanoparticles for removal of Cu(II) ions. *J Colloid Interface Sci* 283: 446–451. https://doi.org/10.1016/j.jcis.2004.09.010
13. Chae HS, Kim SD, Piao SH, et al. (2016) Core-shell Structured Fe_3O_4/SiO_2 Nanoparticles Fabricated by Sol–gel Method and Their Magnetorheology. *Colloid Polym Sci* 294: 647–655. https://doi.org/10.1007/s00396-015-3818-y
14. Li N, Gao P, Chen H, et al. (2022) Amidoxime modified Fe_3O_4/TiO_2 particles for antibacterial and efficient uranium extraction from seawater. *Chemosphere* 287: 132137. https://doi.org/10.1016/j.chemosphere.2021.132137
15. Zhao Y, Li J, Zhao L, et al. (2014) Synthesis of amidoxime-functionalized Fe_3O_4/SiO_2 core-shell magnetic microspheres for highly efficient sorption of U(VI). *Chem Eng J* 235: 275–283. https://doi.org/10.1016/j.cej.2013.09.034
16. Zheng H, Zhou L, Liu Z, et al. (2019) Functionalization of mesoporous Fe_3O_4/SiO_2 nanospheres for highly efficient U(VI) adsorption. *Microporous Mesoporous Mat* 279: 316–322. https://doi.org/10.1016/j.micromeso.2018.12.038
17. Beamish JEC, FE (1948) Uranium, Spectrophotometric Ammonium Thiocyanate Method. *Master analytical manual* 149: 9–12.

18. Werner Stober Af (2017) Controlled Growth of Monodisperse Silica Spheres in the Micron Size Range. *J Phys Ther Sci* 29: 112–114.
19. Kalapathy U, Proctor A, Shultz J (2001) A simple method for production of pure silica from rice hull ash. *Fuel Energy Abstracts* 42: 45. https://doi.org/10.1016/S0140-6701(01)80487-2
20. Pu Y, Qiang T, Li G, et al. (2023) Efficient adsorption of low-concentration uranium from aqueous solutions. *Ecotox Environ Safe* 259: 115053. https://doi.org/10.1016/j.ecoenv.2023.115053
21. Gao B, Gao Y, Li Y (2010) Preparation and chelation adsorption property of composite chelating material poly(amidoxime)/SiO_2 towards heavy metal ions. *Chem Eng J* 158: 542–549. https://doi.org/10.1016/j.cej.2010.01.046
22. Bulut VN, Arslan D, Ozdes D, et al. (2010) Preconcentration, separation and spectrophotometric determination of aluminium(III) in water samples and dialysis concentrates at trace levels with 8-hydroxyquinoline-cobalt(II) coprecipitation system. *J Hazard Mater* 182: 331–336. https://doi.org/10.1016/j.jhazmat.2010.06.034
23. Grimaldi F, May I, Mary F, et al. (1954) Collected Papers on Methods of Analysis for Uranium and Thorium. *Geol Sur Bull* 1006: 196.
24. Zhou Y, Li Y, Liu D, et al. (2021) Adsorption optimization of uranium(VI) onto polydopamine and sodium titanate co-functionalized MWCNTs using response surface methodology and a modeling approach. *Colloid Surf A-Physicochem Eng Asp* 627. https://doi.org/10.1016/j.colsurfa.2021.127145
25. Aurich A, Hofmann J, Oltrogge R, et al. (2017) Pseudo-second order model for sorption processes Y.S. *Org Process Res Dev* 21: 866–870. https://doi.org/10.1021/acs.oprd.7b00090
26. Wijaya AR, Semedi B, Lusiana RA, et al. (2019) Metal contents and Pb isotopes in the surface seawater of the Gulf of Prigi, Indonesia: Detection of anthropogenic and natural sources. *J Braz Chem Soc* 30: 915–929. https://doi.org/10.21577/0103-5053.20180228
27. Suci CW, Wijaya AR, Santoso A, et al. (2020) Fe leaching in the sludge sediment of the prigi beach with tessier-microwave method. *AIP Conference Proceedings* 2231. https://doi.org/10.1063/5.0002589
28. Zhang A, Uchiyama G, Asakura T (2005) PH Effect on the uranium adsorption from seawater by a macroporous fibrous polymeric material containing amidoxime chelating functional group. *React Funct Polym* 63: 143–153. https://doi.org/10.1016/j.reactfunctpolym.2005.02.015
29. Zhao Y, Li J, Zhang S, et al. (2014) Amidoxime-functionalized magnetic mesoporous silica for selective sorption of U(vi). *RSC Adv* 4: 32710–32717. https://doi.org/10.1039/C4RA05128A

AIMS Press